THE JOURNAL OF BIOLOGICAL CHEMISTRY VOL. 287, NO. 1, pp. 748–756, January 2, 2012

Intra-membrane Oligomerization and Extra-membrane Oligomerization of Amyloid-β Peptide Are Competing Processes as a Result of Distinct Patterns of Motif Interplay*

Received for publication, July 11, 2011, and in revised form, November 2, 2011 Published, JBC Papers in Press, November 21, 2011, DOI 10.1074/jbc.M111.281295

Yi-Jiong Zhang[1], **Jing-Ming Shi**[1], **Cai-Juan Bai, Han Wang, Hai-Yun Li, Yi Wu**[2], **and Shang-Rong Ji**[3]

From School of Life Sciences, Lanzhou University, Lanzhou 730000, China

Background: It is currently unclear whether soluble oligomers of the amyloid-β peptide (Aβ) can cause neurotoxicity by direct membrane incorporation.
Results: Aβ monomers but not the soluble oligomers readily insert into the membrane followed by self-assembly into membrane-embedded oligomers.
Conclusion: Solution-phase oligomerization and membrane insertion of Aβ are mutually exclusive processes that proceed through distinct pathways.
Significance: The competing intra- and extra-membrane oligomerization of Aβ may determine distinct neurotoxic mechanisms.

Soluble oligomers of amyloid-β peptide (Aβ) are emerging as the primary neurotoxic species in Alzheimer disease, however, whether the membrane is among their direct targets that mediate the downstream adverse effects remains elusive. Herein, we show that multiple soluble oligomeric Aβ preparations, including Aβ-derived diffusible ligand, protofibril, and zinc-induced Aβ oligomer, exhibit much weaker capability to insert into the membrane than Aβ monomer. Aβ monomers prefer incorporating into membrane rather than oligomerizing in solution, and such preference can be reversed by the aggregation-boosting factor, zinc ion. Further analyses indicate that the membrane-embedded oligomers of Aβ are derived from rapid assembly of inserted monomers but not due to the insertion of soluble Aβ oligomers. By comparing the behavior of a panel of Aβ truncation variants, we demonstrate that the intra- and extra-membrane oligomerization are mutually exclusive processes that proceed through distinct motif interplay, both of which require the action of amino acids 37–40/42 to overcome the auto-inhibitory interaction between amino acids 29–36 and the N-terminal portion albeit via different mechanisms. These results indicate that intra- and extra-membrane oligomerization of Aβ are competing processes and emphasize a critical regulation of membrane on the behavior of Aβ monomer and soluble oligomers, which may determine distinct neurotoxic mechanisms.

Alzheimer disease (AD)[4] is the most common cause of dementia characterized by extracellular amyloid plaques and intracellular neurofibrillary tangles (1, 2). The major component of amyloid plaque is aggregated amyloid-β peptide (Aβ) with a length of 39–43 residues. Aβ is a secreted peptide generated by sequential processing of amyloid precursor protein by β- and γ-secretases. Accumulating *in vitro*, *in vivo*, and genetic evidence indicates that Aβ is causally involved in the pathogenesis of AD, forming the basis of the prevalent amyloid cascade hypothesis (3, 4). The Aβ aggregates, in particular the low molecular weight soluble oligomers, are emerging as the primary toxic species (1, 2, 5, 6). Indeed, pathogenic Aβ soluble oligomers have been isolated from AD-affected human (7, 8) and mouse model (9) brains, and the cerebrospinal fluid level of Aβ oligomers is considered to be a highly promising biomarker for AD diagnosis (10).

Interaction with the cell membrane has been proposed as one of the key mechanisms for Aβ to exert its neurotoxicity (11–13). For example, the membrane can promote aggregation of Aβ monomers, while after incorporating into the membrane, Aβ is able to form channel-like oligomers (14, 15) or even disrupt membrane integrity (16, 17) resulting in cell dysfunction. Although membrane insertion, oligomerization, and neurotoxicity of Aβ appear to be tightly coupled, the correlation between soluble and membrane-embedded oligomers of Aβ remains elusive. In addition, it is currently unclear whether soluble Aβ oligomers can act by direct membrane incorporation.

In the present study, we have characterized the interaction of membrane with Aβ in multiple assembly states and conclude that solution-phase oligomerization and membrane insertion of Aβ are mutually exclusive processes. Our results further

* This work was supported by the National Nature Science Foundation of China (Grants 30970605 and 30930024), the Ministry of Education of China (Grants 20100211110006, 121108 and 109155), the Ministry of Science and Technology of China (Grant 2011CB910500), and Lanzhou University (Grants lzujbky-2012-k18 and lzujbky-2010-k03).
[1] Both authors contributed equally to this work.
[2] To whom correspondence may be addressed: Life Science Building, Room 227, Lanzhou University, Lanzhou 730000, China. Tel./Fax: 86-931-891-4102; E-mail: wuy@lzu.edu.cn.
[3] To whom correspondence may be addressed: Life Science Building, Room 227, Lanzhou University, Lanzhou 730000, China. Tel./Fax: 86-931-891-4176; E-mail: jsr@lzu.edu.cn.

[4] The abbreviations used are: AD, Alzheimer disease; Aβ, amyloid-β peptide; ADDL, Aβ-derived diffusible ligand; PF, protofibril; DPPC, 1,2-dipalmitoyl-*sn*-glycero-3-phosphocholine; DOPC, 1,2-dioleoyl-*sn*-glycero-3-phosphocholine; DPPS, 1,2-dipalmitoyl-*sn*-glycero-3-phospho-L-serine; HFIP, 1,1,1,3,3,3-hexafluoroisopropanol; ThT, thioflavin T; N2a, Neuro-2a mouse neuroblastoma cell; mN, millinewton; aa, amino acid(s); Tricine, *N*-[2-hydroxy-1,1-bis(hydroxymethyl)ethyl]glycine.

indicate that the intra- and extra-membrane oligomerization of Aβ proceed via distinct pathways and may determine separate neurotoxic mechanisms. These results not only reveal an important regulation of membrane on the behavior of Aβ but may provide clues for designing stage-specific and Aβ-targeted therapy.

EXPERIMENTAL PROCEDURES

Reagents—Recombinant Aβ1–42, Aβ1–40, synthetic scrambled Aβ1–42, and fluorescein-labeled Aβ1–42 were purchased from rPeptide (Athens, GA). Synthetic Aβ1–28, Aβ1–36, Aβ11–42, Aβ17–42, and tetramethylrhodamine-labeled Aβ1–42 were purchased from AnaSpec (San Jose, CA). 1,2-Dipalmitoyl-*sn*-glycero-3-phosphocholine (semisynthetic) (DPPC) and 1,2-dipalmitoyl-*sn*-glycero-3-phospho-L-serine (sodium salt) (DPPS) were purchased from Sigma. GM1 ganglioside (brain, ovine ammonium salt), 1,2-dioleoyl-*sn*-glycero-3-phosphocholine (DOPC), cholesterol, sphingomyelin (brain, porcine) were obtained from Avanti Polar Lipids (Alabaster, AL). DPPS was prepared in chloroform/methanol/water (65/30/5, vol%) at 1 mg/ml; all other lipids were dissolved in chloroform/methanol (75/25, vol%) to 1 mg/ml.

Monomeric Aβ Preparation—Aβ monomer free of aggregation was prepared as described with minor modification (18). Lyophilized Aβ was stored in sealed glass vial at −80 °C. After equilibrated for 30 min at room temperature, Aβ was dissolved to 1 mM in 1,1,1,3,3,3-hexafluoro-2-propanol (HFIP, Sigma) by extensive vortex. The peptide was further incubated at 4 °C for 2 h with continuous shaking (~70 rpm) and stored in small aliquots at −80 °C after evaporating off HFIP by N_2 stream. Immediately prior to experiments, the HFIP-treated peptide aliquot was re-suspended to 5 mM in anhydrous dimethyl sulfoxide (DMSO, Sigma) by brief vortex followed by water batch sonication (1 min each).

Oligomeric and Fibrillar Aβ Preparation—For preparation of the low molecular weight soluble oligomer Aβ-derived diffusible ligand (ADDL), 100 μM monomeric Aβ was incubated in F-12 medium (Ham's F-12, BioSource, Australia) for 24 h at 4 °C (18, 19). Aβ protofibril (PF) was prepared by incubating 100 μM Aβ monomer in TBS (50 mM Tris, 100 mM NaCl, pH 7.4) for 24 h at room temperature followed by 14,000 × *g* centrifugation to remove large aggregates (11, 20, 21). Aβ fiber was prepared by incubating 500 μM Aβ monomer in TBS for 2 weeks at room temperature and pelleted by centrifugation at 14,000 × *g*.

Langmuir Film Balance—Monolayer experiments were conducted with a μTrough-S microbalance (Kibron, Finland) as described previously (22). Lipids were spread onto the TBS buffer (10 mM Tris, 140 mM NaCl, pH 7.4) filled in the trough to achieve a stable initial surface pressure (π_i). Aβ was injected into the subphase to a final concentration of 600 nM through the side hole. The membrane pressure (π) was monitored at intervals of 1 s until a stable value was reached, usually within 5000 s. The measurements were performed at a temperature of 23.5 ± 0.5 °C with continuous stirring. In a typical assay with a constant surface area, the increase in surface pressure of monolayer ($\Delta\pi$) reflects the membrane insertion of Aβ. Linear fitting of $\Delta\pi$ *versus* π_i yields a straight line with negative slope, which intersects the *x* axis at the critical membrane insertion pressure (π_c). π_c represents the highest surface pressure of a monolayer below which a protein can insert, thereby quantitatively defining the membrane insertion capacity. The surface pressure of physiological lipid bilayer is ~30–32 millinewtons (mN)/m (23–24), indicating that a protein can insert into cell membrane only when its π_c is >30 mN/m. To detect the aggregation state of monolayer inserted Aβ, experiments were conducted with a constant surface pressure, and Aβ insertion would result in surface area expansion. After 5000 s, monolayers were collected into tubes via negative pressure produced by vacuum for immunoblotting.

Liposome Experiments—Large unilamellar liposomes were prepared using a mini-extruder (Avanti) as described previously (22). After incubation of Aβ with liposomes for the indicated times, a 10-min centrifugation at 14,000 × *g* was conducted to pellet large Aβ aggregates. The resulting supernatant was subjected to additional centrifugation and SDS-PAGE analysis as indicated in Fig. 3*A*. In some experiments, a 30-min treatment with acidic buffer (1 M NaCl, 20 mM NaH_2PO_4, pH 2.0 adjusted by acetic acid) was used to dissociate low affinity interaction of Aβ with liposomes. In cross-linking experiments, PBS was used instead of TBS. Alternatively, Aβ was mixed with DPPC in chloroform at a molar ratio of 1:200. The mixture was dried under an N_2 stream and resuspended in 10 mM TBS (pH 7.4) to 1 mg/ml of lipid concentration. Then a 20-min bath sonication was used to prepare reconstituted proteoliposome with integrated Aβ (25).

Electrophoresis and Immunoblotting—Aβ samples were separated on 4% to 16.5% gradient of Tris-Tricine SDS-PAGE (1% SDS), transferred to a polyvinylidene difluoride membrane (GE Healthcare) by a semi-dry trans-blot device (Bio-Rad), and probed with mAb 6E10 (Signet) or 4G8 (Millipore, MA) (1:5000, 2 h, room temperature). 5% fat-free milk was used to block the membrane. Antibodies were diluted in TBS, 0.05% Tween 20, 1% BSA. ECL (Pierce) was used to visualize the Aβ signal. In some experiments, before SDS-PAGE samples were cross-linked with a 50-fold molar excess of freshly prepared bis(sulfosuccinimidyl) suberate (Pierce) for 10 min at room temperature followed by quenching with 1 M Tris (pH 7.4) for 15 min.

FRET Assay—Fluorescein (0.5 μM)-labeled Aβ (donor) and 0.5 μM tetramethylrhodamine-labeled Aβ (acceptor) were co-incubated with liposomes at the indicated peptide/lipid ratio with continuous stirring under room temperature. An LS-55 fluorometer (PerkinElmer Instruments) was used to detect the fluorescence emission at 588 and 540 nm (5 nm slit width) with an excitation wavelength of 470 nm (2.5 nm slit width). The FRET ratio was calculated as $F_{A(588\ nm)}/F_{D(540\ nm)}$, where $F_{A(588\ nm)}$ and $F_{D(540\ nm)}$ represent acceptor and donor emission intensities, respectively.

EM—A 5-μl droplet of Aβ sample (~45 μg/ml) was added to a freshly glow-discharged carbon-coated EM grid for 1 min followed by staining with 1% sodium phosphotungstate for 30 s. The grids were examined with a Tecnai G20 (FEI) transmission EM.

ThT Fluorescence—1 μM Aβ samples were incubated with 5 μM thioflavin T (ThT) for 15 min. ThT fluorescence was deter-

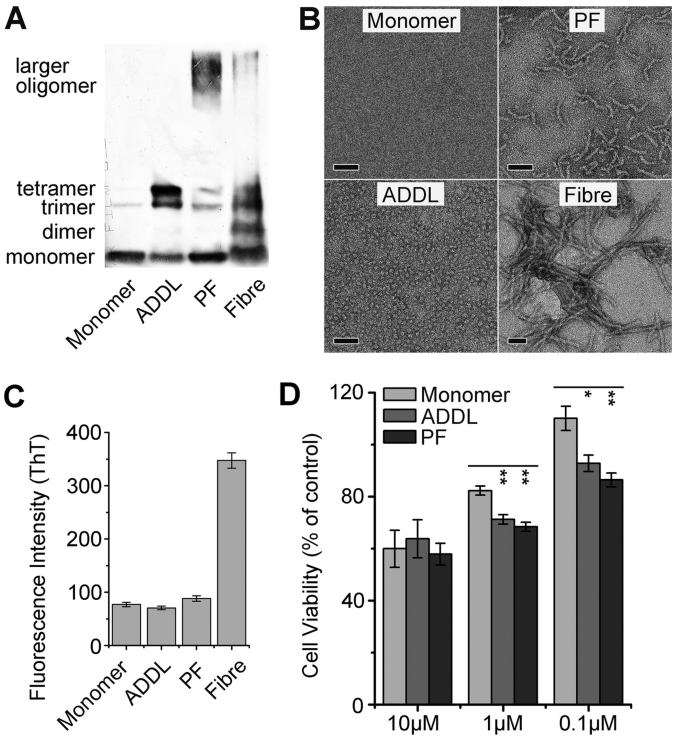

FIGURE 1. **Characterization of Aβ samples in different assembly states.** The characteristics of Aβ monomer, ADDL, protofibril (*PF*), and fiber were assessed by immunoblotting with 6E10 (*A*), EM observation (*scale bars* represent 50 nm) (*B*), and thioflavin T (*ThT*) fluorescence (*C*). Aβ monomer primarily migrated as a single band at ~4.5 kDa in SDS-PAGE and was invisible under EM, whereas ADDL was characterized by bands corresponding to trimer/tetramer in SDS-PAGE and particle-like appearances with even size distribution (~5 nm) under EM. There were additional high molecular weight bands in PF and fiber, and these two samples showed expected morphology. The absence of fiber in Aβ monomer, ADDL, and PF preparations were further verified by the comparable low ThT fluorescence as compared with that of mature fiber. *D*, cell viability of N2a cells treated with different sterile Aβ species for 48 h was assessed by 3-(4,5-dimethylthiazol-2-yl)-2,5-diphenyltetrazolium bromide assay. Results ($n > 3$) are given as mean ± S.E.; *, $p < 0.05$; **, $p < 0.005$. At low concentrations PF and ADDL are significantly more toxic than monomer sample in cell viability assay.

mined by using an LS-55 fluorometer (PerkinElmer; Ex 440 nm/Em 490 nm).

Cell Viability—Neuro-2a (N2a) mouse neuroblastoma cells were cultured in DMEM supplemented with 100 units/ml penicillin, 100 mg/ml streptomycin, and 10% heat-inactivated FBS at 37 °C, 5% CO_2. Aβ was incubated with N2a cells for 48 h in DMEM, 1% FBS. At the end of incubation, 3-(4,5-dimethylthiazol-2-yl)-2,5-diphenyltetrazolium bromide was added to 0.25 mg/ml for 2 h. Cell viability was assessed by $A_{570\ nm}$.

RESULTS

The more amyloidgenic isoform Aβ1–42 was used and is referred to as Aβ hereafter in the subsequent experiments unless otherwise stated. To investigate the interaction of soluble Aβ oligomers with membrane, we prepared and carefully characterized four Aβ samples in different assembly states, *i.e.* monomer, low molecular weight soluble oligomer (ADDL, Aβ-derived diffusible ligand), PF, and mature fiber following the established protocols (11, 18–20). These Aβ species exhibited expected features in SDS-PAGE, EM observation, ThT fluorescence, and cytotoxicity assays (Fig. 1 and its legend) (11, 18–20, 26).

Soluble Aβ Oligomers Exhibit Impaired Membrane Insertion Capability—We examined Aβ-membrane interactions by using Langmuir film balance, which measures changes in surface pressure of lipid monolayer as an index of protein insertion. The term of "insertion" here means part of the tested molecule is incorporated into the hydrophobic core of monolayer resulting in the increase in monolayer surface pressure. The injection of Aβ monomer evoked an abrupt rise of the surface pressure of DPPC monolayer (Fig. 2*A*), reflecting a strong insertion of Aβ monomer. By contrast, the addition of fiber resulted in only marginal changes, whereas ADDL and PF induced moderate surface pressure increases and required longer time to reach the equilibrium. Increasing the amount of injected ADDL did not rescue the insertion defects. Similar findings were also obtained with DPPS and lipid raft (a lipid raft-mimic component)-mimic monolayers (Fig. 2, *B* and *C*). Further quantitative analysis revealed that the Aβ monomer possessed a ~1.5- to 4-fold higher affinity for lipid monolayer and ~1.5-fold stronger maximal monolayer insertion than ADDL (Fig. 2*D*). These findings indicated that prior oligomerization in solution impaired the intrinsic capability of Aβ in membrane insertion regardless of lipid composition. Because the lateral pressure of physiological lipid bilayer is ~30 mN/m (23, 24), the lower values of the critical membrane insertion pressure (π_c) (Fig. 2*E*) suggest that ADDL is unable to directly insert membrane bilayer. Consistent with this speculation, after a 2-h co-incubation with liposomes ADDL still resided in solution phase, whereas Aβ monomer was primarily found to be associated with liposomes (Fig. 2*F*). The above results demonstrate that soluble Aβ oligomers exhibit impaired insertion capability and low affinity to membrane and emphasize that incomplete monomerization of Aβ will lead to an underestimation of the membrane insertion capacity.

Membrane-inserted Aβ Monomers undergo Rapid Oligomerization—Remarkably, incubating 1 μM Aβ monomers with liposomes resulted in rapid occurrence of membrane-associated oligomers that co-sedimented with liposomes in ultracentrifugation, whereas no self-assembly could be observed for Aβ monomers incubated alone (Fig. 3*A*). FRET assay using Aβ monomers tagged with fluorescein and tetramethylrhodamine further revealed a fast kinetics of membrane-induced oligomerization showing almost no lag time (Fig. 3*B*). The Aβ oligomers were not dissociated from liposomes by harsh acidic treatment (Fig. 3*A*), suggesting they were membrane-embedded. Indeed, their assemble pattern was essentially identical as that of the channel-like oligomers within membrane prepared directly from Aβ-lipid fusion mixtures (Fig. 3*C*) (25). Because the soluble Aβ oligomer, *i.e.* ADDL, was unable to associate with liposomes (Fig. 2, *E* and *F*), the intra-membrane oligomers should derive from the assembly of inserted Aβ monomers instead of the insertion of Aβ oligomers formed in solution or on membrane surface. Accordingly, the interaction of Aβ monomers with monolayer did not follow the pattern of simple insertion; instead it fitted well with a two-phase process (Fig. 3*D*). The early and late phases most likely represent the initial insertion and the subsequent intra-membrane conformational change or oligomerization, respectively. Consistent with this speculation, the monolayer-inserted Aβ was largely oligomeric, whereas in

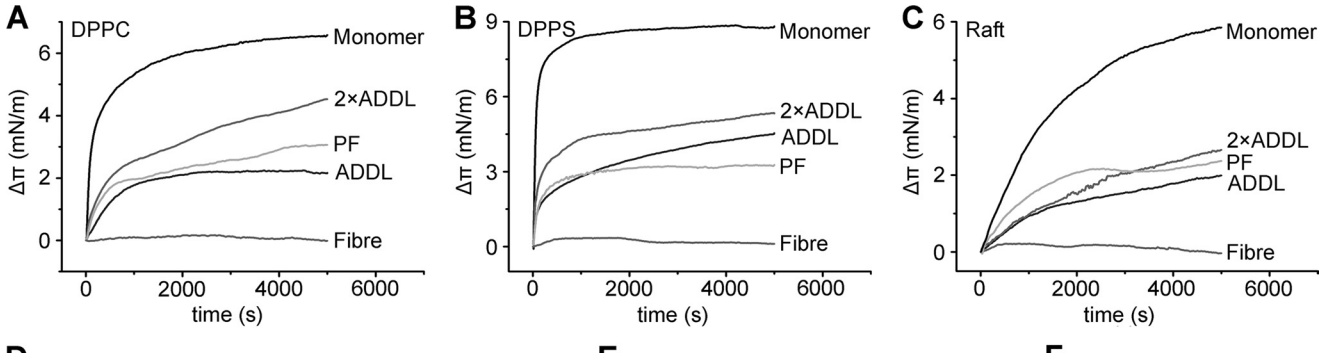

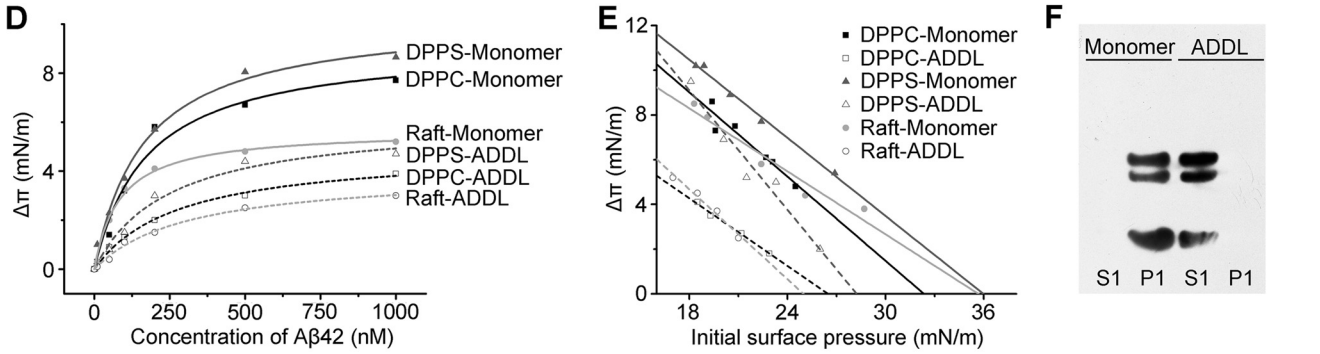

	$\Delta\pi_{max}$		K_d	
	Monomer	ADDL	Monomer	ADDL
DPPC	9.21	4.87	172.8	277.5
DPPS	10.31	6.14	164.7	246.1
Raft	5.68	3.97	83.6	310.4

π_c	Monomer	ADDL
DPPC	32.35	26.48
DPPS	35.98	28.23
Raft	35.67	24.98

FIGURE 2. **Solution-phase oligomerization impairs membrane insertion of Aβ.** *A–C*, 600 nM Aβ monomer, ADDL (1200 nM for 2×ADDL), protofibril, or fibril was injected into the subphase beneath DPPC, DPPS or lipid raft-mimic monolayers with an initial surface pressure of 22 ± 1 mN/m, and the surface pressure increase ($\Delta\pi$) − time curves were recorded. Raft-mimic monolayer was composed of DOPC, sphingomyelin, cholesterol, and GM1 ganglioside with a mole ratio of 32:32:31:5. Injection of Aβ monomer evoked an abrupt increase in surface pressure, whereas a slow and moderate increase was induced by addition of ADDL and PF. These indicate that Aβ monomer exhibited much stronger membrane insertion capability than ADDL and PF. Mature fiber was essentially unable to insert monolayer. *D*, surface pressure increases of lipid monolayers with an initial surface pressure of 22 ± 1 mN/m evoked by Aβ monomer or ADDL at the indicated concentrations. The data were fitted by the Hill equation ($n = 1$), and the corresponding parameters were listed in the *inset table*. These quantitative analyses indicate Aβ monomer possesses significantly higher affinity and maximal insertion capacity than ADDL. *E*, surface pressure change ($\Delta\pi$) − initial surface pressure (π_i) plots of Aβ interaction with monolayers composed of different lipids. The values of critical insertion pressure (π_c) of Aβ for these monolayers are listed in the *inset table*. Because the π_c of ADDL is lower than 30 mN/m, the physiological lateral pressure of cell membrane, this suggests that, unlike Aβ monomer, ADDL is unable to directly insert membrane bilayer. *F*, 1 μM Aβ monomer or ADDL was incubated with 200 μM DPPC liposomes for 2 h at room temperature. Aβ in the liposome-bound (*P1*) and supernatant fractions (*S1*; please refer to the *scheme* shown in Fig. 3*A* for the detailed preparation protocol) were obtained by ultracentrifugation at 200,000 × *g* for 30 min and probed by immunoblotting with 6E10. Aβ monomer was detected only in the liposome fraction while ADDL was exclusively detected in the solution fraction.

the subphase Aβ remained monomeric (Fig. 3*E*). A scrambled Aβ control, on the other hand, exhibited only one-phase membrane insertion.

Intra- and Extra-membrane Oligomerization of Aβ Are Competing Processes—An interesting feature of the interaction between Aβ monomer and membrane was that, at non-saturating low concentration (1:200 molar ratio; 1 μM), essentially all peptide translocated to liposomes with no detectable signal of Aβ monomer or oligomer left in the solution fraction (Fig. 3*A*). This suggests that Aβ monomers prefer membrane association to oligomerization in solution at least at low micromolar concentration. However, the presence of aggregation-boosting factor, *i.e.* zinc ion (27) (Fig. 4*A*), nearly abrogated the membrane insertion of Aβ monomer, although it did not suppress the surface pressure increase evoked by Aβ17–42, an N-terminal truncated isoform without the zinc binding site (28) (Fig. 4*B*). As comparison, another bivalent ion, calcium, was much less potent than zinc in promoting Aβ self-assembly, and only marginally inhibited membrane insertion of Aβ monomer as expected. Nonetheless, the addition of zinc after Aβ incorporation into monolayer failed to reverse the insertion. These findings indicate that solution-phase oligomerization and membrane insertion of Aβ are competitive in nature, which is also in line with the observed inverse correlation between the aggregation extent and insertion capacity (Fig. 2).

Because Aβ monomers and soluble Aβ oligomers, such as ADDL, are more or less in continuous interconversion (29, 30), we reasoned that the preferential incorporation of Aβ monomers into membrane might gradually shift the equilibrium of monomers ↔ ADDL transition, thereby leading to the accumulation and oligomerization of Aβ in liposomes. Indeed, although ADDL showed no detectable membrane association after a 2-h incubation (Figs. 2*F* and 4*C*), prolonged incubation (6–48 h) of ADDL with liposomes resulted in the occurrence of membrane-associated Aβ in liposome fraction (Fig. 4*C*) that was resistant to acidic striping (Fig. 4*D*) despite the fact that most of ADDL still remained in solution phase as observed by EM (Fig. 4*E*). Moreover, the slow accumulation of Aβ oligo-

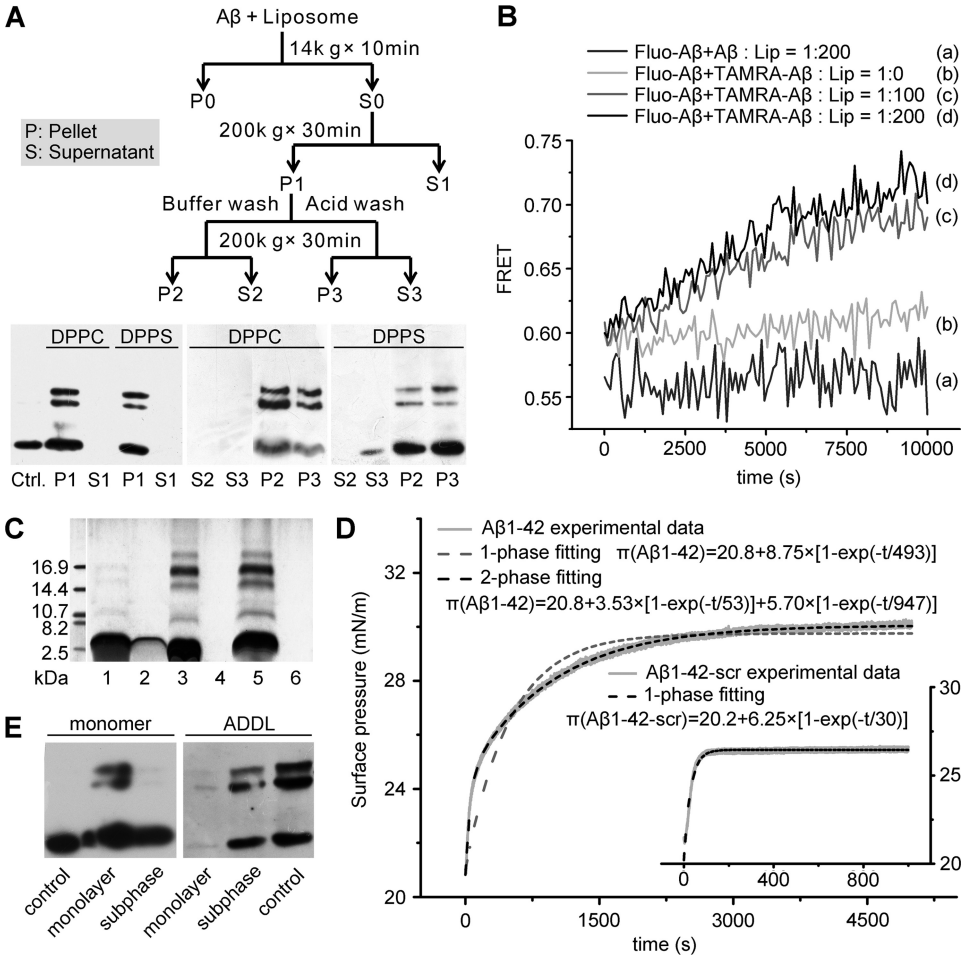

FIGURE 3. **Membrane-associated Aβ monomers undergo rapid oligomerization.** *A*, 1 μM Aβ monomer was incubated with 200 μM DPPC or DPPS liposomes for 2 h at room temperature and further processed as indicated in the scheme. Aβ in the liposome-bound (*P*: pellet) and supernatant fractions (*S*: supernatant) with or without acidic buffer treatment were detected by immunoblotting with 6E10. The *Ctrl. lane* is Aβ monomer, which underwent identical treatment in the absence of liposomes. Almost all the Aβ monomers were sedimented with liposomes, and acid treatment was unable to release liposome-associated Aβ. *B*, 0.5 μM fluorescein-labeled monomeric Aβ (donor) and 0.5 μM tetramethylrhodamine (*TAMRA*)-labeled monomeric Aβ (acceptor) were co-incubated with liposomes at the indicated peptide/lipid ratios, and FRET signal was collected and calculated as described under "Material and Methods." The rapid increase in FRET signal indicates membrane-induced efficient oligomerization of Aβ. By contrast, no FRET signal could be detected when liposomes were absent or unlabeled peptide was used as acceptor. *C*, membrane-associated Aβ oligomers were prepared by reconstituting Aβ-lipid fusion mixture (1:200 molar ratio) or incubating Aβ monomer with the preformed liposomes (1:200 molar ratio). Samples were cross-linked with bis(sulfosuccinimidyl) suberate before silver-staining SDS-PAGE. *Lanes 1* and *2* are Aβ monomer controls without lipid or liposomes. *Lanes 3* and *4* are pellet and supernatant fractions of reconstituted Aβ-lipid fusion sample, respectively. *Lanes 5* and *6* are pellet and supernatant fractions of liposome-Aβ incubation sample, respectively. It was evident that the two samples showed similar self-assembly patterns. *D*, exponential fitting of π-t plots of Aβ monomer insertion into DPPC monolayer. The experimental data of wild-type Aβ insertion deviates from one-phase process fitting but fits well to a two-phase process, suggesting that after insertion Aβ undergoes further conformational changes. As a comparison, the kinetics of scrambled Aβ fit better to a one-phase process. *E*, 600 nM Aβ monomer or ADDL was injected into the subphase beneath DPPC with a constant surface pressure of 28 mN/m. After 5000 s, the monolayer and subphase fractions were separated for subsequent immunoblotting with 6E10. The *control lane* is the Aβ monomer or ADDL at the same concentration incubating for 5000 s. The monolayer-inserted Aβ was largely oligomeric while Aβ in the subphase remained monomeric.

mers in liposomes (Fig. 4*C*) suggests that they were formed by gradual intra-membrane assembly by inserted Aβ monomers but not direct incorporation of ADDL. Therefore, we conclude that the extra- and intra-membrane oligomerization (or membrane insertion) of Aβ are competing processes (Fig. 4*F*).

Distinct Pathways of Intra- and Extra-membrane Assembly of Aβ—To dissect the mechanism of the intra-membrane oligomerization, we further analyzed the interactions of a panel of Aβ variants with membrane (Fig. 5, *A* and *B*). Aβ1–28, the N-terminal extracellular portion of Aβ, was unable to insert both monolayer and bilayer, highlighting the importance of the C-terminal trans-membrane portion of Aβ1–42 in mediating membrane insertion. Indeed, even a short truncation in the C-terminal of Aβ1–42 impaired its interaction with membrane as evidenced by the abrogated and moderately reduced liposome association of Aβ1–36 and Aβ1–40, respectively. Given that the two peptides possess sufficient high π_c to insert the physiological bilayer, these results indicate that aa 29–36 are likely to be the basic unit for metastable/reversible membrane insertion of Aβ, whereas aa 37–40/42 are additionally required for firm attachment. Moreover, aa 37–40/42, or a stable membrane integration, appear to be essential for the intra-membrane self-assembly, because Aβ1–42 and Aβ1–40 efficiently oligomerized within membrane, while no liposome-associated Aβ1–36 oligomer could be observed. N-terminal truncations, however, did not impair membrane interactions of Aβ as expected. However, it resulted in a disparate self-assembly pattern: the intra-membrane oligomerization was somewhat

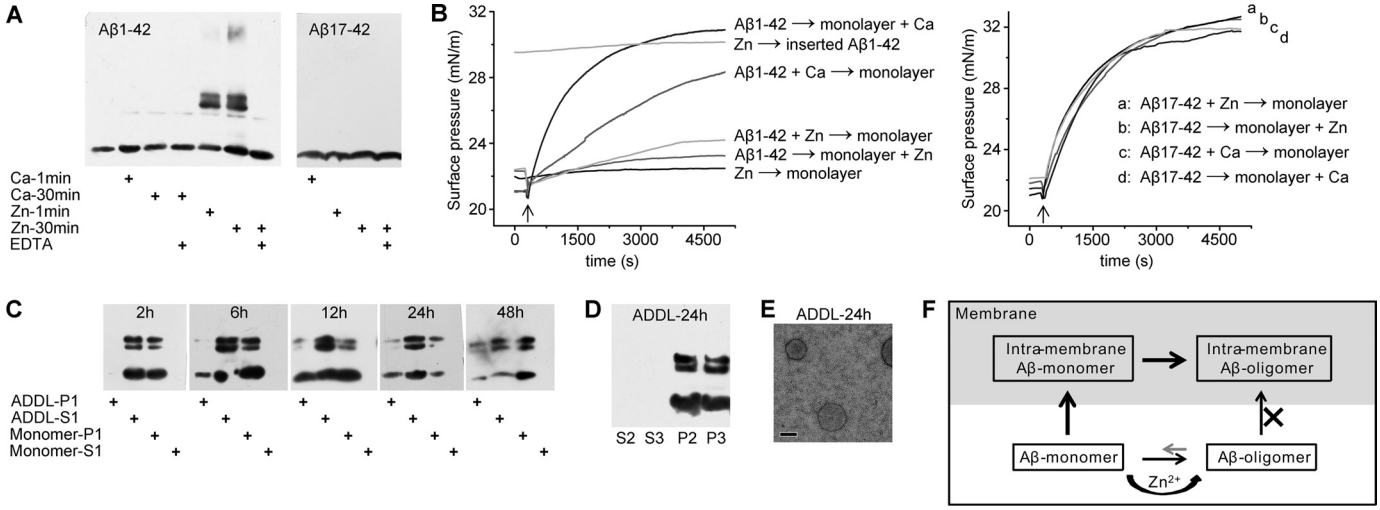

FIGURE 4. **Intra- and extra-membrane oligomerization of Aβ are competing processes.** *A*, the influence of zinc and calcium ions on Aβ oligomerization in solution was assessed by immunoblotting with 6E10 and 4G8 for detection of Aβ1–42 and Aβ17–42, respectively. 50 μM Zn^{2+} markedly accelerated the self-assembly of Aβ1–42 but not Aβ17–42, whereas Ca^{2+} showed little effect. Co-incubation of 100 μM EDTA abrogated the effects of Zn^{2+}. *B*, the influence of zinc and calcium ions on Aβ1–42 or Aβ17–42 monomer insertion into DPPC monolayer. The *arrow* indicates the time of peptide injection. Zinc ion almost abrogated the monolayer insertion of Aβ1–42 irrespective of whether zinc was preincubated with Aβ1–42 or was just present during insertion. By contrast, zinc ion did not affect the insertion of Aβ17–42, a truncated Aβ variant without zinc binding site. Calcium ion showed little effect on Aβ1–42 insertion. *Zn ⟶ monolayer*, injection of Zn^{2+} alone into the metal ion-free subphase; *Aβ1–42 ⟶ monolayer + Zn*, injection of Aβ1–42 alone into the subphase containing Zn^{2+}; *Aβ17–42 ⟶ monolayer + Zn*, injection of Aβ17–42 alone into the subphase containing Zn^{2+}; *Aβ1–42 + Zn ⟶ monolayer*, injection of Aβ1–42 preincubated with Zn^{2+} into the metal ion-free subphase; *Aβ17–42 + Zn ⟶ monolayer*, injection of Aβ17–42 preincubated with Zn^{2+} into the metal ion-free subphase; *Aβ1–42 ⟶ monolayer + Ca*, injection of Aβ1–42 alone into the subphase containing Ca^{2+}; *Aβ17–42 ⟶ monolayer + Ca*, injection of Aβ17–42 alone into the subphase containing Ca^{2+}; *Aβ1–42 + Ca ⟶ monolayer*, injection of Aβ1–42 preincubated with Ca^{2+} into the metal ion-free subphase; *Aβ17–42 + Ca ⟶ monolayer*, injection of Aβ17–42 preincubated with Ca^{2+} into the metal ion-free subphase; *Zn ⟶ inserted Aβ1–42*, injection of Zn^{2+} alone into the metal ion-free subphase beneath the monolayer with prior inserted Aβ1–42. *C*, 1 μM ADDL or Aβ monomer was incubated with DPPC liposomes for the indicated time and the liposome-bound (*P1*) and supernatant fractions (*S1*; please refer to the *scheme* shown in Fig. 3*A* for the detailed preparation protocol) were probed for Aβ signal by immunoblotting with 6E10. ADDL was incubated with DPPC liposomes for 24 h followed by 6E10 immunoblotting of liposome-bound (*P2*) and supernatant fractions (*S2*) after acidic buffer treatment (*D*) or EM observation (*E*). Prolonged incubation of ADDL with liposomes resulted in occurrence of liposome-associated Aβ oligomers, suggesting liposomes gradually shifts the equilibrium of monomers ↔ ADDL interconversion, thereby leading to the accumulation and oligomerization of Aβ in liposomes. The *scale bar* represents 100 nm. *F*, the proposed model depicting the distinct interactions of Aβ monomer and soluble oligomer with membrane. In the absence of aggregation-boosting factors (*e.g.* zinc ion) in solution, Aβ monomers preferentially insert membrane and undergoes rapid intra-membrane oligomerization. Appreciable solution-phase oligomerization may ensue only at elevated Aβ concentrations or with the co-existence of aggregation-boosting factors (*e.g.* zinc) to counteract the avid membrane interaction. Soluble oligomers are unable to insert membrane; rather they may function primarily by binding to high affinity cell surface receptors.

enhanced with Aβ11–42 but completely diminished with Aβ17–42. Therefore, aa 11–16 are responsible for the formation of stable intra-membrane Aβ oligomers. The failure of Aβ17–42 to oligomerize within membrane indicates that the intact C-terminal alone is insufficient in mediating the formation of the stable intra-membrane oligomer. These results thus establish a C-terminal insertion initiated intra-membrane self-assembly pathway that ends up with the N-terminal stabilized oligomers.

We continued to investigate the oligomerization of the above Aβ variants in the absence of liposomes (Fig. 5*C*) to gain further insight into how membrane regulates Aβ self-assembly. 100 μM instead of 1 μM Aβ was used, because without liposomes the aggregation of Aβ is rather inefficient at a low level (16). Remarkably, Aβ1–28 was most prone to aggregation as exemplified by the complete dimerization instantly after the conventional HFIP/DMSO treatment that works well to monomerize Aβ1–42. Extending the C-terminal of Aβ1–28 to 36 resulted in the least aggregative peptide, *i.e.* Aβ1–36, indicating a motif within the sequence of aa 29–36 antagonizes the N-terminal directed Aβ self-assemble. Indeed, such interaction could also explain the inability of aa 29–36 to mediate firm membrane attachment of Aβ (please see under "Discussion"). Further extension of the C-terminal to 40 or 42 led to mild and significant reversion of the aggregation defect of Aβ1–36, respectively. Hence, aa 37–40 and particularly aa 40–42 are able to partially release the inhibition imposed by aa 29–36. Additional experiments identified aa 1–10 as a repressor and aa 11–16 as an important motif in mediating Aβ oligomerization, because the aggregation of Aβ11–42 and Aβ17–42 was enhanced and markedly reduced, respectively. In contrast to the inability of Aβ17–42 to form intra-membrane oligomer, this peptide retained significant self-assembly capability in the absence of liposomes, indicating that one or more motifs other than aa 11–16, most likely the C-terminal, also contribute to the solution-phase oligomerization of Aβ.

Taken together, these results underscore that the self-assembly of Aβ is progressed as a result of complex interplay among multiple motifs in its own sequence. Interestingly, a common initiating event appears to be shared by the extra- and intra-membrane oligomerization, *i.e.* overcoming the auto-inhibition conferred by the interaction between aa 29–36 and the N-terminal portion through the action of aa 37–40/42 albeit via different mechanisms. This would release Aβ into a state permissive for solution self-assembly or stable membrane attachment. However, distinct pathways then ensue for extra- and intra-membrane oligomerization as exemplified by their differential requirement for aa 11–16. Indeed, this motif is exclu-

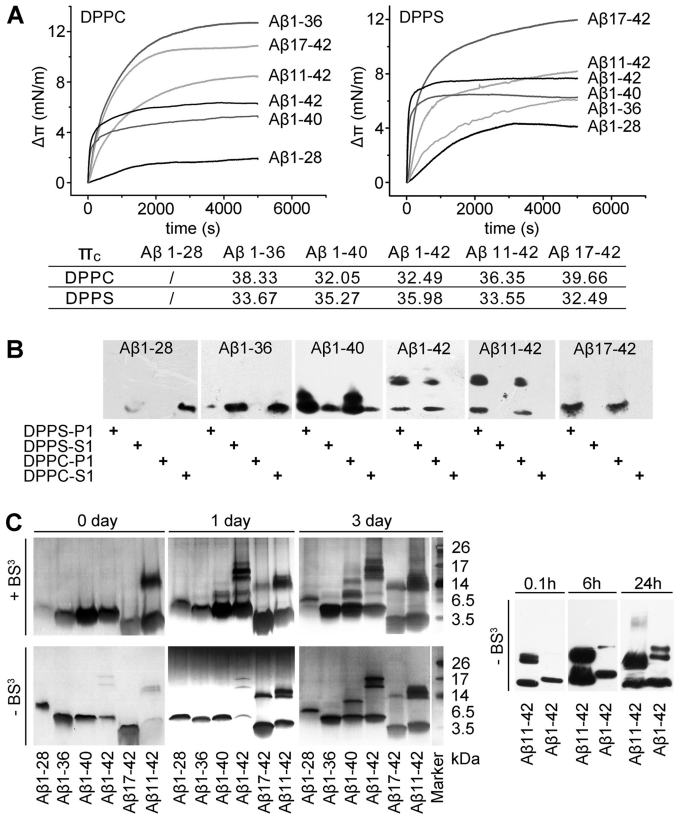

FIGURE 5. **Intra- and extra-membrane assembly of Aβ proceed via distinct pathways.** *A*, the Δπ-t curves of Aβ variant insertion into DPPC and DPPS monolayers with an initial surface pressure of 22 ± 1 mN/m. The values of π_c were also indicated in the *inset table*. Except for Aβ1–28, all other peptides showed sufficient capacity to insert a physiological membrane. *B*, 1 μM Aβ variants were incubated with 200 μM DPPC or DPPS liposomes for 2 h at room temperature. The liposome-bound (*P1*) and supernatant fractions (*S1*; please refer to the *scheme* shown in Fig. 3*A* for the detailed preparation protocol) were probed by immunoblotting with 4G8. Almost no liposome association of Aβ1–28 and Aβ1–36 could be detected, whereas Aβ1–42, Aβ1–40, and Aβ11–42 showed a high level of membrane association and intra-membrane oligomerization. Despite strong membrane association, no intra-membrane oligomer of Aβ17–42 was observed. *C*, 100 μM Aβ variants were incubated in TBS at room temperature for the indicated times and analyzed by silver-staining SDS-PAGE (the *left panel*) with or without cross-linking, or by immunoblotting with 4G8 (the *right panel*) without prior cross-linking by bis-(sulfosuccinimidyl) suberate (*BS*^{3}). The aggregation patterns in silver-staining SDS-PAGE with or without cross-linking are very similar. At such a high concentration, all the Aβ variants aggregated albeit with different kinetics and capacity. Aβ1–28 is the most aggregative peptide showing no monomeric band in SDS-PAGE, whereas Aβ1–36 is the least aggregative peptide, the majority of which remained monomeric after a 3-day incubation.

sively required for the formation of stable intra-membrane oligomers (Fig. 5*B*) but seems to be somewhat dispensable in the extra-membrane self-assembly (Fig. 5*C*). Hence, except for facilitating the spatial proximity of Aβ molecules non-specifically, membrane insertion also enhances the self-assembly of Aβ1–40/42 through regulating the pattern of motif interplay as these peptides oligomerized much more efficient within membrane than in solution.

DISCUSSION

Soluble Aβ oligomers play an essential role in the pathogenesis of AD (1, 2, 5), however, whether the membrane is among their direct targets that mediate the downstream neurotoxic effects remains elusive. Herein, we show that multiple soluble oligomeric Aβ preparations, including ADDL, PF, and zinc-induced Aβ oligomer, exhibit much weaker capability to insert membrane than that of Aβ monomer (Figs. 2–4), suggesting that solution-phase oligomerization masks the motif responsible for membrane insertion. Indeed, as part of the transmembrane segment of amyloid precursor protein, the C-terminal of Aβ not only mediates membrane insertion (31, 32) but is intimately involved in extra-membrane self-assembly (33–38). As such, it is plausible that these two processes are mutually exclusive, which is further corroborated by our findings that zinc-accelerated solution-phase oligomerization markedly suppresses membrane insertion (Fig. 4). Although some reports propose that soluble Aβ oligomers may alter membrane conductivity by direct insertion (39, 40), the reversibility of such effect by simple washing would, instead, argue for a weak interaction of non-insertion nature. Overall, it may be safe to conclude that stable soluble Aβ oligomers are incapable to insert membrane, although certain (transient) metastable oligomerization intermediates in solution-phase self-assembly pathway might still be competent in membrane insertion, likely due to prominent hydrophobic surface exposure as suggested by Streltsov *et al.* (33) and Nag *et al.* (41).

Aβ monomers appear to prefer membrane incorporation to solution-phase oligomerization at least at a low peptide level (Fig. 3, *A* and *B*). Moreover, following insertion Aβ monomers rapid assemble into oligomers within membrane, which are essentially identical in assembly pattern as channel-like oligomers (Fig. 3*C*). Hence, appreciable solution-phase oligomerization may ensue only with elevated Aβ concentrations or with the co-existence of aggregation-boosting factors (*e.g.* zinc) to counteract the avid membrane interaction. Although the inability of the soluble Aβ oligomer to insert or stably attach to the membrane suggests that this toxic species is unlikely to induce cell dysfunction via direct interacting with the membrane, high affinity cell surface receptors (42, 43) have been identified to bind and mediate the adverse effects of soluble Aβ oligomers. Therefore, the competing intra- and extra-membrane oligomerization of Aβ may determine two distinct toxic mechanisms. The intra-membrane oligomerization of Aβ and the associated compromise of membrane integrity likely dominate in the earliest phase of AD initiation for the less pathogenic microenvironment (*e.g.* low Aβ production and insignificant accumulation of metal ion), whereas with the disease progression the extra-membrane self-assembly will gradually become favorable, and soluble Aβ oligomers may thus play a more prominent role via signaling through cell receptors. Moreover, despite being a vulnerable target membrane may also help to alleviate the acute attack of soluble Aβ oligomers by converting them to the less toxic intra-membrane species (Figs. 1*D*, 3*A*, 4*C*, and 4*F*).

By comparing the extra- and intra-membrane oligomerization behavior of Aβ variants, we are able to gain further insight into the complex interplay among multiple sequence motifs within Aβ underlying the conformational changes associated with its self-assembly (Fig. 5). Remarkably, among the examined peptides, Aβ1–36 emerges as the unique one showing interesting properties. First, Aβ1–36 is very inefficient in self-assembly, despite the fact that Aβ1–28 (44) and aa 25–35 (45) are both highly aggregative in solution. Second, although it

evokes strong pressure increase in monolayer assays, Aβ1–36 fails to stably associate with membrane, despite that the amino acid 30–36 sequence is the most hydrophobic stretch in the sequence of Aβ and aa 25–35 have been reported to insert and form ion channels within the membrane (46, 47). These results thus suggest an antagonistic interaction between aa 29–36 and aa 1–28, the extracellular domain of Aβ. Consistent with this notion, aa 30–36 comprise the most represented segment that constitutes the major part of the C-terminal strand and participates in the intra-molecular β-hairpin formation by pairing the central hydrophobic cluster (aa 17–21) within the N-terminal strand, as revealed by extensive NMR characterization and x-ray crystallography (33–38). Accordingly, such interaction may disable the respective functionalities dictated by the two respective sequences of aa 29–36 and 1–28 and, hence, lock Aβ1–36 in an auto-inhibited configuration.

Extension of the C terminus of Aβ1–36 to 40/42 moderately/markedly rescued the defect in solution-phase oligomerization and stable membrane insertion. Because the strand pairing between aa 30–36 and the central hydrophobic cluster is largely retained as the basic folding unit in the structure models of Aβ resolved under different extra-membrane assembly states (33–38), we propose that, instead of breaking the antagonistic interaction between these two segments, aa 37–40/42 may overcome the self-assembly defect via one of the following mechanisms: (i) it acts in concert with aa 30–36 to form a longer β-hairpin that is more compatible for efficient aggregation as illustrated in the fibril structures (34, 35); or (ii) it provides additional docking site or surface for stable inter-molecular interaction as revealed in the structures of soluble oligomers (33, 36, 38). By contrast, the pairing between aa 30–36 and the central hydrophobic cluster in Aβ1–40/42 is likely to be broken during membrane insertion to allow stable incorporation via the transmembrane portion. Indeed, the intriguing metastable or reversible membrane insertion of Aβ1–36 suggests that the membrane can facilitate the reconfiguration of this peptide (or the hairpin) to expose the membrane-spanning segment (*i.e.* aa 29–36). However, due to the shortened C terminus, there is probably only a small free energy difference between the auto-inhibited solution state and the membrane-inserted state of Aβ1–36, allowing an interconversion between these two states. In monolayer experiments, the excessive amount of peptide and the interconversion equilibrium together allow the existence of a sufficient amount of membrane-inserted peptide in the steady state of insertion. By contrast, in bilayer experiments, during the separation of liposomes from the bulk solution by ultracentrifugation, the decrease in peptide-liposome contact favors the conversion from inserted to auto-inhibited state and, hence, results in depletion of Aβ1–36 from liposomes. As such, the increased hydrophobicity of the longer C terminus of Aβ1–40/42 will further stabilize the inserted conformation leading to more stable membrane incorporation.

Our findings also reveal an important role of the N-terminal hydrophilic portion, *i.e.* aa 1–17, in regulating the self-assembly of Aβ. Deletion of aa 1–10 enhanced both intra- and extra-membrane oligomerization albeit to different extents, indicating Aβ11–42, the amyloidgenic product of the alternative β-secretase pathway, is more prone to oligomerize than Aβ1–42 consistent with its proposed role in the early phase of AD (48). The α-secretase pathway product Aβ17–42, on the contrary, is considered as a non-amyloidgenic isoform. Accordingly, we found this peptide was unable to form stable intra-membrane oligomers and oligomerized in solution with a markedly reduced efficiency. Although the underlying mechanism awaits further exploration, these results pinpoint aa 11–16 as the critical motif in promoting Aβ self-assembly. Paradoxically, Aβ17–42 has recently been reported to form ion channels in lipid bilayer (49). This finding, however, does not necessarily contrast to our results because: (i) the discrepancy may be due to different experimental conditions, such as peptide/lipid ratio (~1/15 *versus* 1/200) and peptide level (10–40 μM *versus* 1 μM); (ii) the dynamic assembly and disassembly of the channel observed by Jang *et al.* (49) are indicative of a weak inter-molecular interaction, which is in agreement with the inability of Aβ17–42 to form the stable intra-membrane oligomer identified herein. Together, our current work emphasizes a critical regulation of membrane on the behavior of Aβ monomer and soluble oligomers, which may have implications in understanding the role of Aβ in AD pathology.

REFERENCES

1. Citron, M. (2010) *Nat. Rev. Drug Discov.* **9,** 387–398
2. Golde, T. E., Schneider, L. S., and Koo, E. H. (2011) *Neuron* **69,** 203–213
3. Hardy, J., and Selkoe, D. J. (2002) *Science* **297,** 353–356
4. Hardy, J. A., and Higgins, G. A. (1992) *Science* **256,** 184–185
5. Haass, C., and Selkoe, D. J. (2007) *Nat. Rev. Mol. Cell Biol.* **8,** 101–112
6. Zhang Lan, Y. Y., and Wang, C. (2010) *Acta Biophys. Sin.* **26,** 649–661
7. Shankar, G. M., Li, S., Mehta, T. H., Garcia-Munoz, A., Shepardson, N. E., Smith, I., Brett, F. M., Farrell, M. A., Rowan, M. J., Lemere, C. A., Regan, C. M., Walsh, D. M., Sabatini, B. L., and Selkoe, D. J. (2008) *Nat. Med.* **14,** 837–842
8. Jin, M., Shepardson, N., Yang, T., Chen, G., Walsh, D., and Selkoe, D. J. (2011) *Proc. Natl. Acad. Sci. U.S.A.* **108,** 5819–5824
9. Lesné, S., Koh, M. T., Kotilinek, L., Kayed, R., Glabe, C. G., Yang, A., Gallagher, M., and Ashe, K. H. (2006) *Nature* **440,** 352–357
10. Hampel, H., Frank, R., Broich, K., Teipel, S. J., Katz, R. G., Hardy, J., Herholz, K., Bokde, A. L., Jessen, F., Hoessler, Y. C., Sanhai, W. R., Zetterberg, H., Woodcock, J., and Blennow, K. (2010) *Nat. Rev. Drug Discov.* **9,** 560–574
11. Kayed, R., Head, E., Thompson, J. L., McIntire, T. M., Milton, S. C., Cotman, C. W., and Glabe, C. G. (2003) *Science* **300,** 486–489
12. Glabe, C. G. (2006) *Neurobiol. Aging* **27,** 570–575
13. Axelsen, P. H., Komatsu, H., and Murray, I. V. (2011) *Physiology* **26,** 54–69
14. Quist, A., Doudevski, I., Lin, H., Azimova, R., Ng, D., Frangione, B., Kagan, B., Ghiso, J., and Lal, R. (2005) *Proc. Natl. Acad. Sci. U.S.A.* **102,** 10427–10432
15. Arispe, N., Rojas, E., and Pollard, H. B. (1993) *Proc. Natl. Acad. Sci. U.S.A.* **90,** 567–571
16. Ege, C., and Lee, K. Y. (2004) *Biophys. J.* **87,** 1732–1740
17. Ambroggio, E. E., Kim, D. H., Separovic, F., Barrow, C. J., Barnham, K. J., Bagatolli, L. A., and Fidelio, G. D. (2005) *Biophys. J.* **88,** 2706–2713
18. Stine, W. B., Jr., Dahlgren, K. N., Krafft, G. A., and LaDu, M. J. (2003) *J. Biol. Chem.* **278,** 11612–11622
19. Lambert, M. P., Barlow, A. K., Chromy, B. A., Edwards, C., Freed, R., Liosatos, M., Morgan, T. E., Rozovsky, I., Trommer, B., Viola, K. L., Wals, P., Zhang, C., Finch, C. E., Krafft, G. A., and Klein, W. L. (1998) *Proc. Natl. Acad. Sci. U.S.A.* **95,** 6448–6453
20. Walsh, D. M., Hartley, D. M., Kusumoto, Y., Fezoui, Y., Condron, M. M., Lomakin, A., Benedek, G. B., Selkoe, D. J., and Teplow, D. B. (1999) *J. Biol. Chem.* **274,** 25945–25952
21. Martins, I. C., Kuperstein, I., Wilkinson, H., Maes, E., Vanbrabant, M.,

Jonckheere, W., Van Gelder, P., Hartmann, D., D'Hooge, R., De Strooper, B., Schymkowitz, J., and Rousseau, F. (2008) *EMBO J.* **27,** 224–233
22. Ji, S. R., Ma, L., Bai, C. J., Shi, J. M., Li, H. Y., Potempa, L. A., Filep, J. G., Zhao, J., and Wu, Y. (2009) *FASEB J.* **23,** 1806–1816
23. Marsh, D. (1996) *Biochim. Biophys. Acta* **1286,** 183–223
24. Seelig, A. (1987) *Biochim. Biophys. Acta* **899,** 196–204
25. Lin, H., Bhatia, R., and Lal, R. (2001) *FASEB J.* **15,** 2433–2444
26. Jan, A., Hartley, D. M., and Lashuel, H. A. (2010) *Nat. Protoc.* **5,** 1186–1209
27. Bush, A. I., Pettingell, W. H., Multhaup, G., d.'Paradis, M., Vonsattel, J. P., Gusella, J. F., Beyreuther, K., Masters, C. L., and Tanzi, R. E. (1994) *Science* **265,** 1464–1467
28. Minicozzi, V., Stellato, F., Comai, M., Dalla Serra, M., Potrich, C., Meyer-Klaucke, W., and Morante, S. (2008) *J. Biol. Chem.* **283,** 10784–10792
29. Bitan, G., Lomakin, A., and Teplow, D. B. (2001) *J. Biol. Chem.* **276,** 35176–35184
30. Nag, S., Sarkar, B., Bandyopadhyay, A., Sahoo, B., Sreenivasan, V. K., Kombrabail, M., Muralidharan, C., and Maiti, S. (2011) *J. Biol. Chem.* **286,** 13827–13833
31. Liu, R. Q., Zhou, Q. H., Ji, S. R., Zhou, Q., Feng, D., Wu, Y., and Sui, S. F. (2010) *J. Biol. Chem.* **285,** 19986–19996
32. Ji, S. R., Wu, Y., and Sui, S. F. (2002) *J. Biol. Chem.* **277,** 6273–6279
33. Streltsov, V. A., Varghese, J. N., Masters, C. L., and Nuttall, S. D. (2011) *J. Neurosci.* **31,** 1419–1426
34. Paravastu, A. K., Leapman, R. D., Yau, W. M., and Tycko, R. (2008) *Proc. Natl. Acad. Sci. U.S.A.* **105,** 18349–18354
35. Lührs, T., Ritter, C., Adrian, M., Riek-Loher, D., Bohrmann, B., Döbeli, H., Schubert, D., and Riek, R. (2005) *Proc. Natl. Acad. Sci. U.S.A.* **102,** 17342–17347
36. Yu, L., Edalji, R., Harlan, J. E., Holzman, T. F., Lopez, A. P., Labkovsky, B., Hillen, H., Barghorn, S., Ebert, U., Richardson, P. L., Miesbauer, L., Solomon, L., Bartley, D., Walter, K., Johnson, R. W., Hajduk, P. J., and Olejniczak, E. T. (2009) *Biochemistry* **48,** 1870–1877
37. Hoyer, W., Grönwall, C., Jonsson, A., Ståhl, S., and Härd, T. (2008) *Proc. Natl. Acad. Sci. U.S.A.* **105,** 5099–5104
38. Ahmed, M., Davis, J., Aucoin, D., Sato, T., Ahuja, S., Aimoto, S., Elliott, J. I., Van Nostrand, W. E., and Smith, S. O. (2010) *Nat. Struct. Mol. Biol.* **17,** 561–567
39. Sokolov, Y., Kozak, J. A., Kayed, R., Chanturiya, A., Glabe, C., and Hall, J. E. (2006) *J. Gen. Physiol.* **128,** 637–647
40. Valincius, G., Heinrich, F., Budvytyte, R., Vanderah, D. J., McGillivray, D. J., Sokolov, Y., Hall, J. E., and Lösche, M. (2008) *Biophys. J.* **95,** 4845–4861
41. Nag, S., Chen, J., Irudayaraj, J., and Maiti, S. (2010) *Biophys. J.* **99,** 1969–1975
42. Laurén, J., Gimbel, D. A., Nygaard, H. B., Gilbert, J. W., and Strittmatter, S. M. (2009) *Nature* **457,** 1128–1132
43. Cissé, M., Halabisky, B., Harris, J., Devidze, N., Dubal, D. B., Sun, B., Orr, A., Lotz, G., Kim, D. H., Hamto, P., Ho, K., Yu, G. Q., and Mucke, L. (2011) *Nature* **469,** 47–52
44. Klajnert, B., Cortijo-Arellano, M., Cladera, J., and Bryszewska, M. (2006) *Biochem. Biophys. Res. Commun.* **345,** 21–28
45. Millucci, L., Raggiaschi, R., Franceschini, D., Terstappen, G., and Santucci, A. (2009) *J. Biosci.* **34,** 293–303
46. Mason, R. P., Estermyer, J. D., Kelly, J. F., and Mason, P. E. (1996) *Biochem. Biophys. Res. Commun.* **222,** 78–82
47. Qi, J. S., and Qiao, J. T. (2001) *Neuroscience* **105,** 845–852
48. Liu, K., Solano, I., Mann, D., Lemere, C., Mercken, M., Trojanowski, J. Q., and Lee, V. M. (2006) *Acta Neuropathol.* **112,** 163–174
49. Jang, H., Arce, F. T., Ramachandran, S., Capone, R., Azimova, R., Kagan, B. L., Nussinov, R., and Lal, R. (2010) *Proc. Natl. Acad. Sci. U.S.A.* **107,** 6538–6543